Transition from local to global phase synchrony in small world neural network and its possible implications for epilepsy

Bethany Percha, Rhonda Dzakpasu, and Michał Żochowski
Department of Physics and Biophysics Research Division, University of Michigan, Ann Arbor, Michigan 48109, USA

Jack Parent
Department of Neurology, University of Michigan Medical School, Ann Arbor, Michigan 48109, USA
(Received 12 November 2004; revised manuscript received 3 June 2005; published 16 September 2005)

Temporal correlations in the brain are thought to have very dichotomous roles. On one hand they are ubiquitously present in the healthy brain and are thought to underlie feature binding during information processing. On the other hand, large-scale synchronization is an underlying mechanism of epileptic seizures. In this paper we show a potential mechanism for the transition to pathological coherence underlying seizure generation. We show that properties of phase synchronization in a two-dimensional lattice of nonidentical coupled Hindmarsh-Rose neurons change radically depending on the connectivity structure of the network. We modify the connectivity using the small world network paradigm and measure properties of phase synchronization using a previously developed measure based on assessment of the distributions of relative interspike intervals. We show that the temporal ordering undergoes a dramatic change as a function of topology of the network from local coherence strongly dependent on the distance between two neurons, to global coherence exhibiting a larger degree of ordering and spanning the whole network.

DOI: 10.1103/PhysRevE.72.031909 PACS number(s): 87.18.Hf, 05.45.Xt, 05.65.+b, 87.19.La

I. INTRODUCTION

Epilepsy is a common neurological disorder characterized by spontaneous recurrent seizures. Epileptic seizures are generated by indiscriminate, synchronized bursting of multiple cortical neurons [1], leading to increased coherence in the recorded signal between individual neurons as well as throughout whole networks [2,3]. A wide range of molecular and cellular mechanisms, including alterations in ion channels and neurotransmitter receptors, may underlie seizure generation; however, most abnormalities are thought to result in increased excitatory transmission mediated by N-methyl-D-aspartic acid (NMDA), alpha-amino-3–hydroxy-5–methyl-4–isoxazolepropionic acid (AMPA), or metabotropic glutamate receptors, or decreased inhibitory gamma-aminobutyric acid (GABA-ergic) transmission, causing an imbalance between cortical excitation and inhibition [4]. The potential network mechanisms proposed to underlie excessive excitatory neurotransmission during epileptogenesis include loss of inhibitory interneurons and aberrant axonal sprouting (reviewed in [5]). For example, mesial temporal lobe epilepsy, the most common form of refractory partial epilepsy, is associated with aberrant axonal reorganization of excitatory dentate granule cell axons (mossy fibers) onto neighboring granule neurons (reviewed in [6]). Evidence suggests that mossy fiber sprouting leads to abnormal recurrent excitation that may be critical for seizure initiation or propagation in this network [7].

Studies of rodent mesial temporal lobe epilepsy models have shown that structural network remodeling during epileptogenesis leads to significant increases in axonal length as compared to intact neuronal networks [8]. We hypothesize that hyperexcitability induced by sprouting could be one of the causes of synchronous discharges underlying seizures, and show that alteration of the network topology produces a relatively abrupt transition in phase/lag coherence in the two-dimensional (2D) small world network (SWN) lattice of nonidentical Hindmarsh-Rose (H-R) models of thalamocortical neurons [9]. Furthermore, our results indicate that the observed abrupt transition has all the hallmarks of a phase transition. We also show that around the transition point (in terms of network topology) as the network switches from one to the other dynamical regime, the durations of the coherent (globally synchronized) phase scales like a power law having exponent of $a=-1.557$ indicating that type III intermittency is a dynamical mechanism underlying this global transition. This latest result coincides with experimental ones showing similar properties of the distributions of seizure durations [10,11].

Emergence of the concept of small-world networks [12] has allowed for rigorous study of the properties of intermediate-structured networks where the connectivities are neither entirely regular nor entirely random. In those networks the rewiring parameter P controls the topology of the network: when $P=0$ only local connections are present, and conversely if $P=1$ any two neurons in the network can be connected with the same probability (global connectivity). Networks exhibiting such structure have been identified in social as well as biological systems [12,13]. Most studies have concentrated on their static properties [14–16]. However, recent work has also focused on the dynamic properties of SWN, including synchronization. It has been shown that the linear stability of the synchronous state is linked to the algebraic condition of the Laplacian matrix defining network topology [17,18]. It has been reported that this synchronized state is achieved in SWN more efficiently (in terms of required network connectivity) than standard deterministic graphs, purely random graphs, and ideal constructive

schemes [19]. It has also been shown that small-world networks of interconnected Hodgkin-Huxley neurons combine two features: rapid and large oscillatory response to the stimulus [20]. Properties of self-sustained activity have also been studied in the SWN of excitable neurons [21].

II. DEFINITION OF THE STUDIED NETWORK

Here we study the emergence of temporal interdependencies in a (SW) network of coupled nonidentical H-R neurons. It has been established that periodically driven nonlinear oscillators or a system of coupled nonidentical oscillators can achieve phase or, with stronger coupling, time-lag synchronization [22–27]. The equations of the H-R neurons are

$$\dot{x}_i = y_i - ax_i^3 + bx_i^2 - z_i + I_{0_i} + \frac{\alpha}{K}\sum_{j,\|i,j\|\leq R}(x_j - x_i),$$

$$\dot{y}_i = c - dx_i^2 - y_i,$$

$$\dot{z}_i = r[s(x_i - x_0) - z_i]. \tag{1}$$

The x, y, and z coordinates represent membrane potential, fast current, and slow current, respectively. Initially, all neurons within radius R are connected via bidirectional coupling having strength α. Those connections are then randomly modified with probability P, with each original bidirectional connection being treated as two unidirectional connections that can move independently. The 12×12 lattice has periodic boundary conditions (i.e., torus topology); the lattice constant (distance between nearest neighbors) is set to unity. The neural parameters in the above equations are $a=1.0$, $b=3.0$, $c=1.0$, $d=5.0$, $r=0.006$, $s=4.0$, and $x_0=-1.6$; K is the number of actual connections per neuron. The parameter I_{0_i} represents the amplitude of external current applied to the ith neuron and determines the frequency as well as type of the dynamical regime of the neuron (periodic, bursting, and/or chaotic). The $I_{0_i} \in [2.5, 3.4]$, and were generated at random, ensuring that they had nonidentical properties.

III. ADAPTIVE MEASUREMENT OF COHERENCE CHANGES IN THE NETWORK

We use our previously developed measure ([28]) to monitor asymmetric properties of phase or lag synchronization in the lattice. The measure monitors the properties of the relative interspike intervals (ISI) between neuronal pairs [Fig. 1(a)]. This allows us to interpret the temporal interdependencies between the coupled units in terms of relative interspike timings.

Specifically the interspike interval Δt_m^{ij} of the jth unit with respect to the ith neuron is calculated as a time difference between the spike time of the jth neuron and the last spike of the ith neuron that directly preceeds it, and conversely the interspike interval Δt_m^{ji} of the ith neuron is calculated as a time difference between the spike of neuron i and the timing of the last spike fired by the jth neuron that directly preceeds it. Thus, if t_1^i, t_2^i are the spike timings fired by the ith neuron, t_1^j, t_2^j are the spike timings fired by the jth neuron, and t_1^i

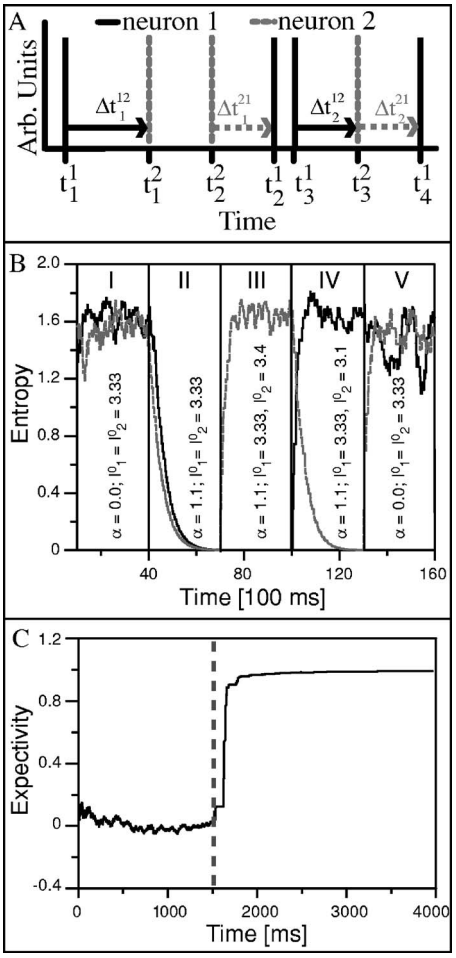

FIG. 1. (a) Individual distributions are updated for every neuron using the relative durations of the ISI of every neuron with respect to the other in the pair (for all the possible pairs in the network). Specifically, the ISI Δt_m^{ij} of the jth neuron with respect to the ith neuron is calculated as a time difference between the spike timing of the jth neuron with respect to the last spike of the ith neuron, and conversely the ISI Δt_m^{ji} of the ith neuron is calculated as a time difference between the spike of neuron i with respect to the timing of the last spike taking place on the jth neuron. The distributions are updated every time a new spike is generated. (b) Changes in the phase lag (as measured by CEs) in response to changes in the relative values of I_{0_i} for a system two H-R neurons. (1) Initially the neurons are uncoupled ($\alpha=0$) with the same control parameters ($I_{0_i}=3.3$). Both of the CEs are high (no phase synchronization is present). (2) After 40 s the coupling is introduced ($\alpha=1.1$). The CE of both neurons converges to zero indicating complete synchronization. (3) After another 40 ms the value of $I_{0_2}=3.4$. The CE with respect to neuron 1 is high, whereas the other one is zero indicating phase synchronization with neuron 1 lagging behind neuron 2. (4) After another 40 s the control parameters are modified so that $I_{0_1}=3.33$ and $I_{0_2}=3.1$ reversing that of the previous case. The CE calculated with respect to neuron 2 is high, whereas the other one is zero indicating that neuron 2 is now lagging behind neuron 1. (5) Finally, we return to $\alpha=0$ and any phase relations are abolished. (c) Changes in the expectivity function for fully connected network of H-R neurons. The dashed line denotes time at which coupling was turned on ($\alpha=1.1$).

$> t_1^j > t_2^i > t_2^j$, then one distribution will be updated with only one interspike interval ($\Delta t^{ji} = t_2^i - t_1^j$) whereas the second distribution will be updated twice with ($\Delta t^{ij} = t_1^j - t_1^i$) and ($\Delta t^{ij} = t_2^j - t_2^i$). The distributions defined in this manner are complementary to each other, providing complete information about possible asymmetric timing interdependencies between the coupled units.

The ISIs are calculated for every neuron pair in the network separately as new spikes are generated. The distributions are updated dynamically throughout the simulation, so that if the interspike interval created at time (t) falls within a time window described by bin I, the probability assigned to that bin becomes $P_I(t) = P_I(t-1) + \Delta P$; ΔP is the free parameter of the measure and determines its dependence on the previous ISIs. After every update, the ISI distributions are renormalized and their Shannon entropy $S = -\Sigma_I P_I \ln P_I$, is calculated. Since the distributions depend on the relative timings of spikes of both neurons in the pair, we refer to them as conditional entropies (CEs). Since the relative ISI are measured unidirectionally [Fig. 1(a)], the measure provides a time dependent assessment of the instantaneous interdependencies between the neurons, while the pairwise comparison of CEs allows for asymmetric measurement of temporal interdependencies between any two neurons in the network. Those two characteristics of the measure make it directly applicable to experimental data.

As a result an $N \times N$ conditional entropy matrix is formed for all neurons in the network, with elements (i,j) and (j,i) providing information about the temporal interdependencies appearing at a given time of the neural pairs in the network. In the ideal situation the (S_{ij}, S_{ji}) pair can take four distinctly different values [Fig. 1(b)]:

- $S_{ij} \simeq S_{ji} \neq 0$. This indicates that the interspike distributions of both neurons are fairly wide and they are not phase locked—their dynamics are uncorrelated.
- $S_{ij} \simeq 0$ and $S_{ji} \neq 0$. This implies that the ijth distribution is somewhat narrow whereas the jith distribution is wide. The two neurons are locked with the jth neuron having a persistent lag relative to the ith neuron.
- $S_{ij} \neq 0$ and $S_{ji} \simeq 0$. This implies the reverse situation—that the jith distribution is somewhat narrow whereas the ijth distribution is wide—the ith neuron has a persistent lag relative to the jth neuron.
- $S_{ij} \simeq S_{ji} \simeq 0$. Both distributions are peaked. This usually implies complete synchronization of both neurons.

Measures using relative interspike intervals have been defined before [29] however the advantage of the measure presented here is the fact that it provides asymmetrical and dynamical assessment of changing temporal correlations in the network.

The lag between two nonidentical neurons established during phase/lag synchronization depends on their relative properties (i.e., intrinsic frequencies) [22,23]. The neuron having higher firing frequency (higher I_{0_i}) will lead that of the neuron having lower spiking frequency [Fig. 1(b)]. If a global synchronous state is reached there will be global ordering of the lags between the neurons according to their internal parameters (namely, I_0).

Thus we can define an expectivity function that compares the temporal interdependencies in the network to the relative properties of the neurons (the value of I_{0_i})

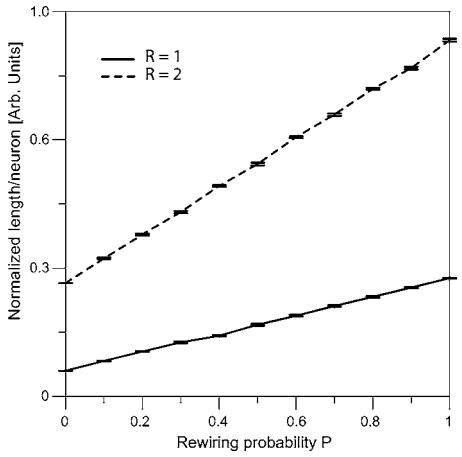

FIG. 2. Changes in the total connection length per neuron as a function of rewiring probability P and the initial connectivity. The average connection length per neuron increases linearly with the rewiring probability. This can be indirectly linked to the experimental result that axonal sprouting leads to significantly increased (up to 30–40 %) axonal length.

$$E = \frac{1}{N(N-1)} \sum_{i,j,i \neq j}^{N} w_{ij}, \tag{2}$$

where

$$w_{ij} = \begin{cases} 1 & \text{if } (S_{ij} - S_{ji})(I_{0_j} - I_{0_i}) > 0 \\ -1 & \text{if } (S_{ij} - S_{ji})(I_{0_j} - I_{0_i}) \leqslant 0 \end{cases}. \tag{3}$$

The S_{ij} is the CE of relative ISI of neuron j with respect to neuron i. Their difference $(S_{ij} - S_{ji})$ will provide a direct assessment of which neuron in the pair is leading and which one is lagging. The expectivity function itself measures the existence of global temporal ordering in the system: namely, whether the direction of the phase lag (i.e., the order of the firing within the pair) is in agreement with that predicted from the relative values of the parameters (I_0) of the neurons (if the value from a given pair is predicted correctly the function is assigned the value $w_{ij} = 1$, and conversely if the prediction fails $w_{ij} = -1$). Thus, if $E \to 1$ this indicates that there is a global order in the temporal sequences of neuronal activities, whereas if no ordering is established $E \simeq 0$ [Fig. 1(c)].

IV. RESULTS

We have used the expectivity function to measure properties of phase synchronization in a sparsely coupled 2D lattice of $N = 12 \times 12 = 144$ networked H-R neurons. The final topology of the network is determined by the rewiring probability P within a small world network (SWN) paradigm. The rewiring probability P was varied from 0 (full local connectivity within the radius R) to 1 (random graph). The radius $R = 1, 2, 3$ defines a cellular distance within which a given neuron forms connections with other neurons, and thus determines the connectivity fraction (number of neurons connected to a given neuron over the number of all the possible

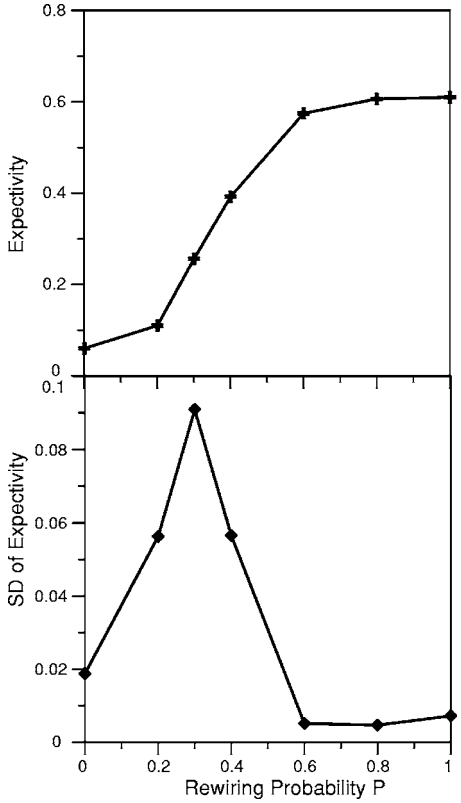

FIG. 3. (a) Expectivity function for different values of rewiring parameter P. For low values of P expectivity values are low indicating a low degree of temporal ordering. Expectivity increases significantly around $P=0.3$ to saturate around the value of 0.8 for higher P. (b) Standard deviation of the expectivity increases dramatically around the transition point of $P=0.3$.

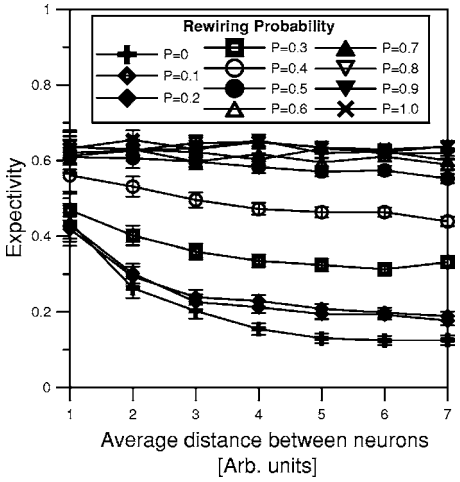

FIG. 4. Changes in the expectivity as a function of neuronal distance for different rewiring probabilities. The temporal ordering remains local for low values of P (expectivity declines as a function of neuronal distance), whereas global phase synchronization is obtained for $P>0.3$. Additionally, for high values of P the degree of phase locking is greater overall than that observed for local phase synchrony. The graph is formed by binning the values of expectivity for all neural pairs that have Euclidean distance within the noted distance range; $\alpha=2.0$, $R=2$. Every point on the graph is an average over four trials.

connections to that neuron) in the network (0.028, 0.083, 0.194, respectively). In addition to the changes of statistical properties of the connectivity, the changes in rewiring probability also significantly increase the total connection length per neuron (Fig. 2)—similar to the effect observed experimentally during sprouting [8].

With an increase in the P value, there is a rapid transition from a disordered state to an ordered state (one where the network is globally synchronized). Moreover, the observed transition has the basic properties of a phase transition and the expectivity function acts as an order parameter.

Figure 3(a) shows the behavior of the expectivity function for different values of the rewiring probability P. For low values of P expectivity is low, indicating only residual temporal ordering in the system which may be due to the finite size of the network. Around $P=0.3$ the expectivity increases dramatically and saturates indicating a transition from a temporally disordered to a globally ordered state. At the same time, the standard deviation [Fig. 3(b)] of the expectivity increases by almost one order of magnitude around $P=0.3$. This is a defining characteristic of a phase transition: Fluctuations of the order parameter near the transition point are expected to increase dramatically.

Furthermore, we have created histograms of the expectivity of all neuron pairs in the network as a function of their relative Euclidean distance on the lattice. This allowed us to infer the local as well as global properties of the temporal ordering in the network and estimate its correlation length. We have observed that for low values of P the temporal relations are preserved over only short distances and the expectivity over longer distances quickly converges to zero. However, as P increases, global ordering is achieved in the network (Fig. 4). Moreover, neurons in random networks ($P=1$) achieve a significantly higher degree of temporal locking than that achieved even for short spatial distances in the networks with low P (Fig. 2). This indicates that the correlation length in the network increases to infinity.

The abruptness of the transition from local phase synchrony to global phase synchrony depends on the connectivity as well as the coupling constant. To depict those changes, we have plotted the average decay ratio of the expectivity as a function of rewiring probability

$$D_{R,\alpha}(P) = \frac{E_{R,\alpha}(L=1,P=0) - E_{R,\alpha}(L=\max,P)}{E_{R,\alpha}(L=1,P=0)}, \quad (4)$$

where $E_{R,\alpha}(L,P)$ is the expectivity averaged over all neuronal pairs having average distance L, computed for the network with rewiring probability P, radius R, and coupling strength α; due to periodic boundary conditions, the maximum distance used in the network is 7. Positive values of the decay (D) indicate local phase synchrony, whereas $D \simeq 0$ indicates global phase synchrony in the network. Negative values of $D(P)$ indicate that ordering of temporal interdependencies between distant neurons for large values of P is more complete than the ordering on the short spatial scale observed for $P=0$ (see Fig. 5). For lower values of alpha there is no significant increase in the degree of global ordering

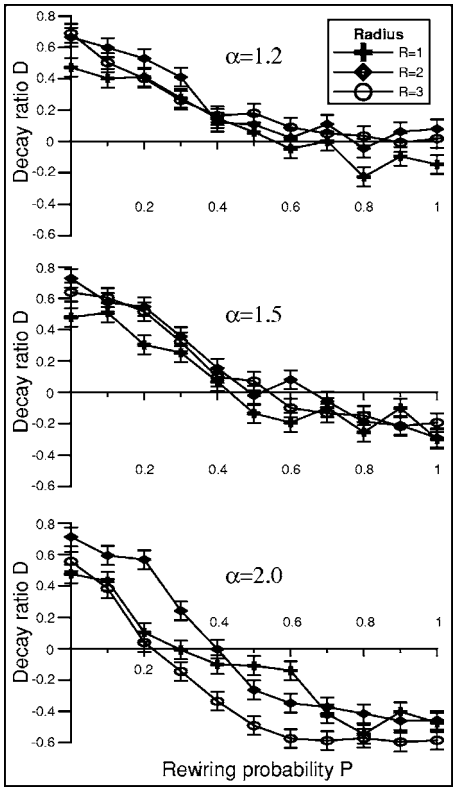

FIG. 5. Average synchrony decay ratio D as a function of rewiring probability P (see definition in the text). Positive values of D indicate large decay and thus local phase synchrony; for $D \simeq 0$ there is no attenuation of synchrony over distance (global synchrony state is achieved); $D < 0$ indicates an increased degree of phase locking within the global synchrony state.

over the degree of ordering on shorter spatial scales. When the coupling is increased there is a significant enhancement in the phase synchrony in the network (up to 50%).

To better characterize the type of the transition near the critical point, we investigated the scaling of the durations of the synchronized (i.e., high expectivity) states near the transition point $P=0.3$ (Fig. 6). We have defined those durations to be the times when the network expectivity is above the 60th percentile of the observed expectivity range. We have also investigated other threshold values and observed distributions that looked virtually the same. The distribution of the durations shows a power law scaling for the short "laminar" bursts, whereas it resembles a multiexponential distribution for the longer ones. This result is in agreement with [30,31] where it was shown that an exponential tail will be observed when additional sources of noise are present in the network. Here the noise is due to the fact that the coupled neurons are not identical [32]. Also the finite size of the studied network might have contributed to this effect.

The exponent of the power law portion of the graph is $a = -1.557$ indicating possible type-III intermittency at the transition point. Interestingly, very similar scaling of the actual seizure duration was observed in experimental and human data, indicating the same type of transition from interictal to ictal states [10,11].

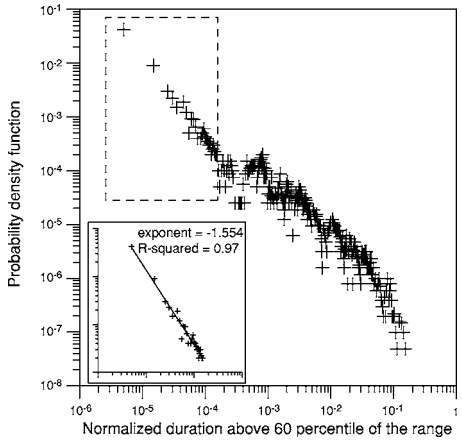

FIG. 6. Scaling of the durations when the network exhibits high expectivity values near the transition point ($P=0.3$). The distribution resembles power law at the short end of the duration and a combination of multiple exponentials at the long end. The inset is the magnification and the fit of the region marked by the dashed box.

V. CONCLUSIONS

In conclusion, we have used our previously developed CE measure to show that a SW network of coupled neurons undergoes an abrupt transition from a disordered temporal state to a globally ordered one. The observed transition has the hallmarks of a phase transition where the rewiring probability P is the control parameter and expectivity is the order parameter. This transition may play an important role in the emergence of certain types of epileptic seizures, as evidence suggests that one of the mechanisms underlying hippocampal seizure generation involves sprouting of glutamatergic processes within this injured brain region. We hypothesize that

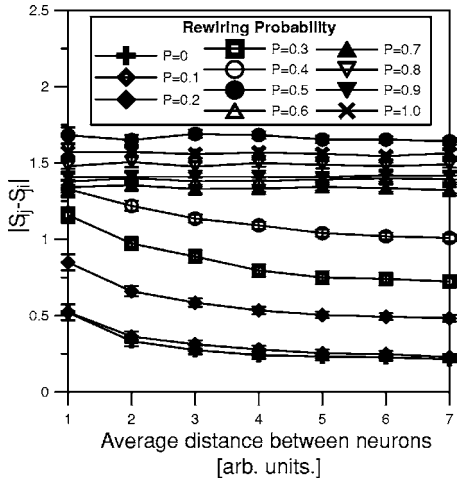

FIG. 7. Changes in $|\Delta S_{ij}|$ as a function of Euclidean distance between the neurons. The entropic differences exhibit the same behavior as the one observed for the expectivity function. This allows the direct application of the measure to the experimental data, where the parameters of the individual neurons cannot be determined. The $|\Delta S_{ij}|$ were calculated for the same parameters as those listed in Fig. 3.

sprouting can cause, over a prolonged period of time, local changes in network connectivity. Those changes in turn could alter the dynamical regime of brain functioning into a parameter regime (near the phase transition point) where rapid switching from one regime to another could take place. The intermittent globally ordered regime would correspond to seizurelike activity.

The critical value of rewiring probability at which the transition takes place fluctuates around $P \simeq 0.3$–0.4. This coincides with the values of P at which the structural clustering coefficient rapidly decays [12]. Moreover, it has been found that the clustering coefficient for *C. elegans*, an example of a completely mapped neural network, is 0.28, which corresponds to a rewiring probability of $P \simeq 0.3$ (assuming perfect SWN structure), indicating that the neural systems may form networks where network structure lies in this critical regime between local and global synchrony. Creation of spurious glutamatergic connections in an injured region (sprouting) may cause the balance to be shifted toward global phase synchrony, leading to the onset of epileptic seizures.

It is interesting to note that by far the most connections are made during brain development. Thus, in view of the results presented here, an underlying mechanism(s) likely exists to control large scale brain topology, that does not permit the brain to reach the seizure-inducing phase but at the same time optimizes its connectivity for the required computation [33,34].

An additional advantage of the devised measure is that it can be applied directly to experimental data. The expectivity function, which cannot be assessed in the case of real data because the internal parameters of individual neurons are not known, can be substituted by pairwise calculation of the average absolute value of entropic differences between individual neurons $|\Delta S_{ij}| = |S_{ij} - S_{ji}|$. The behavior of both measures is virtually the same (Figs. 4 and 7).

ACKNOWLEDGMENT

The authors would like to thank M. Newman for his comments on this work.

[1] C. Deransart, B. Hellwig, M. Heupel-Reuter, J. F. Leger, D. Heck, and C. H. Lucking, Epilepsia **44**, 1513 (2003).
[2] L. M. de la Prida and J. V. Sanchez-Andres, J. Neurophysiol. **82**, 202 (1999).
[3] R. Ferri, C. J. Stam, B. Lanuzza, F. I. Cosentino, M. Elia, S. A. Musumeci, and G. Pennisi, Clin. Neurophysiol. **115**, 1202 (2004).
[4] F. E. Dudek, P. R. Patrylo, and J. P. Wuarin, Adv. Neurol. **79**, 699 (1999).
[5] K. Morimoto, M. Fahnestock, and R. J. Racine, Prog. Neurobiol. **73**, 1 (2004).
[6] J. M. Parent and D. H. Lowenstein, Curr. Opin. Neurol. **10**, 103 (1997).
[7] V. Santhakumar, I. Aradi, and I. Soltesz, J. Neurophysiol. **93**, 437 (2005).
[8] P. S. Buckmaster and F. E. Dudek, J. Neurophysiol. **81**, 712 (1999).
[9] J. L. Hindmarsh and R. M. Rose, Philos. Trans. R. Soc. London, Ser. B **346**, 129 (1994).
[10] J. L. Velazquez and P. L. Carlen, Eur. J. Neurosci. **11**, 4110 (1999).
[11] J. L. Perez-Velazquez and H. Khosravani, Chaos **14**, 333 (2004).
[12] D. J. Watts and S. H. Strogatz, Nature (London) **393**, 440 (1998).
[13] M. E. J. Newman and M. Girvan, Proc. Natl. Acad. Sci. U.S.A. **99**, 2566 (2002).
[14] M. E. J. Newman and D. J. Watts, Phys. Rev. E **60**, 7332 (1999).
[15] M. E. J. Newman, C. Moore, and D. J. Watts, Phys. Rev. Lett. **84**, 3201 (2000).
[16] E. Almaas, R. V. Kulkarni, and D. Stroud, Phys. Rev. Lett. **88**, 098101 (2002).
[17] M. Barahona and L. M. Pecora, Phys. Rev. Lett. **89**, 054101 (2002).
[18] H. Hong, M. Y. Choi, and B. J. Kim, Phys. Rev. E **65**, 026139 (2002).
[19] T. Nishikawa, A. E. Motter, Y. C. Lai, and F. C. Hoppensteadt, Phys. Rev. Lett. **91**, 014101 (2003).
[20] L. F. Lago-Fernandez, R. Huerta, F. Corbacho, and J. A. Siguenza, Phys. Rev. Lett. **84**, 2758 (2000).
[21] A. Roxin, H. Riecke, and S. A. Solla, Phys. Rev. Lett. **92**, 198101 (2004).
[22] M. G. Rosenblum, A. S. Pikovsky, and J. Kurths, Phys. Rev. Lett. **78**, 4193 (1997).
[23] M. G. Rosenblum, A. S. Pikovsky, and J. Kurths, Phys. Rev. Lett. **76**, 1804 (1996).
[24] M. G. Rosenblum, A. S. Pikovsky, G. Osipov, and J. Kurths, Physica D **104**, 219 (1997).
[25] U. Parlitz, L. Junge, W. Lauterborn, and L. Kocarev, Phys. Rev. E **54**, 2115 (1996).
[26] C. Zhou, J. Kurths, I. Z. Kiss, and J. L. Hudson, Phys. Rev. Lett. **89**, 014101 (2002).
[27] D. Pazo, A. M. Zaks, and J. Kurths, Chaos **13**, 309 (2003).
[28] M. Żochowski and R. Dzakpasu, J. Phys. A **37**, 3823 (2004).
[29] D. C. Tam, Biol. Cybern. **78**, 95 (1998).
[30] N. Platt, S. M. Hammel, and J. F. Heagy, Phys. Rev. Lett. **72**, 3498 (1994).
[31] A. Cenys and H. Lustfeld, J. Phys. A **29**, 11 (1996).
[32] A. S. Pikovsky and P. Grassberger, J. Phys. A **24**, 4587 (1991).
[33] D. B. Chklovskii, T. Schikorski, and C. Stevens, Neuron **34**, 341 (2002).
[34] D. B. Chklovskii, Neural Comput. **16**, 2067 (2004).